

Phonon metamorphosis in ferromagnetic manganite films: Probing the evolution of an inhomogeneous state

Ch. Hartinger, F. Mayr, and A. Loidl

EP V, Center for Electronic Correlations and Magnetism, University of Augsburg, 86135 Augsburg, Germany

T. Kopp

EP VI, Center for Electronic Correlations and Magnetism, University of Augsburg, 86135 Augsburg, Germany

(Received 27 December 2004; published 27 May 2005)

The analysis of phonon anomalies provides valuable information about the cooperative dynamics of lattice, spin, and charge degrees of freedom. Significant is the anomalous temperature dependence of the external modes observed in $\text{La}_{2/3}\text{Sr}_{1/3}\text{MnO}_3$ (LSMO) films. The two external modes merge close to the ferromagnetic to paramagnetic transition at T_C and, moreover, two new modes evolve in this temperature range with strong resonances at slightly higher frequencies. We propose that such a phonon metamorphosis probes the inhomogeneous Jahn-Teller distortion, manifest on the temperature scale T_C . The analysis is based on the first observation of all eight phonon modes in the metallic phase of LSMO and on susceptibility measurements which identify a Griffiths-like phase.

DOI: 10.1103/PhysRevB.71.184421

PACS number(s): 75.47.Lx, 72.80.-r, 75.40.Cx, 78.20.-e

The colossal magnetoresistance (CMR) in the manganites is a paradigm of the cooperative dynamics of charge, spin, and lattice degrees of freedom (DOF). Whereas the interplay of charge and spin DOF was realized early on with the discovery of the double exchange (DE) mechanism, the role of the lattice DOF was appreciated only recently: Millis *et al.*¹ argued that the DE alone cannot explain the resistivity data of $\text{La}_{1-x}\text{Sr}_x\text{MnO}_3$. They concluded that a sufficiently strong electron-phonon coupling is responsible for polaronic effects which control the electronic kinetic energy and the resistance peak near the ferromagnetic to paramagnetic transition.

A new perspective was introduced through the notion that the formation of an inhomogeneous state in the vicinity of the transition plays a key role in the CMR phenomenon.²⁻⁴ It not only signifies the competition between the different thermodynamic states which may result from the cooperative dynamics of the considered DOF, but it also emphasizes the relevance of disorder which, through doping, is present in all CMR manganites. In this context, the idea that “CMR is a Griffiths singularity”^{5,6} has been advanced.

Experimental evidence for the presence of inhomogeneous states in the temperature range where the CMR is observed has been reported on many occasions and has been reviewed before (see, for example, Ref. 7). It should be emphasized that the various investigated inhomogeneous states are of different nature although they probably have a common origin which is not yet fully understood. Prominent examples of such investigations are: scanning tunneling spectroscopy^{8,9} which probes the surface states, susceptibility measurements⁵ which display non-Curie-Weiss behavior and refer to competing magnetic states, and neutron-diffraction studies¹⁰ which examine the local Jahn-Teller (JT) distortions related to a microscopic charge distribution.

Most of the previous research focussed on $\text{La}_{1-x}\text{Ca}_x\text{MnO}_3$, as the CMR effect is strongest in the Ca-doped compounds, at $x \approx 1/3$. However, since for these compounds the ferromagnetic to paramagnetic transition (T_C)

nearly coincides with the metal-insulator transition (T_{MIT}), it is of particular relevance to investigate $\text{La}_{1-x}\text{Sr}_x\text{MnO}_3$ where the two temperature scales are different. In this work, we address the observability of the inhomogeneous bulk state through far infrared (FIR) optical spectroscopy in $\text{La}_{2/3}\text{Sr}_{1/3}\text{MnO}_3$ (LSMO) films. We associate phonon anomalies with the formation of the inhomogeneous state. To our knowledge, anomalies of the phononic excitations in LSMO have not been analyzed in the vicinity of the magnetic transition. Probing the inhomogeneous state with phonons should provide insight into the temperature-dependent evolution of electronic correlations which couple to the local lattice structure.

The origin of phononic anomalies may be traced (i) to a strong coupling of phonon modes with an electronic continuum but also (ii) to a modification of the local symmetry, e.g., due to an alteration of the JT distortion. Mechanism (i), which leads to an asymmetric “Fano line shape” of distinct phonons, is observed in $\text{La}_{2/3}\text{Ca}_{1/3}\text{MnO}_3$ films.¹¹ In LSMO films the electron-phonon coupling is much weaker, as evidenced by the polaronic excitations,^{12,13} and correspondingly the asymmetry of the phonon absorption lines is too small to be observable. However, the latter effect (ii), which we denote as “metamorphosis of phonons,” is seen in our LSMO films. The metamorphosis not only includes a temperature dependent frequency shift but, more notably, the merging of phonon lines and the evolution of new resonances. We observe a transfer of spectral weight from the pronounced phonon modes at low temperature into the “new modes” at high temperature. This metamorphosis is controlled by the magnetic temperature scale T_C .

The study of thin films is indispensable in order to resolve the full set of phonon modes even in the metallic low-temperature phase. Enhanced screening in the single crystals suppresses the phonon resonances wherefore the infrared active phonons in $\text{La}_{2/3}\text{Sr}_{1/3}\text{MnO}_3$ have not been investigated in the literature. Apart from rendering the phonons observ-

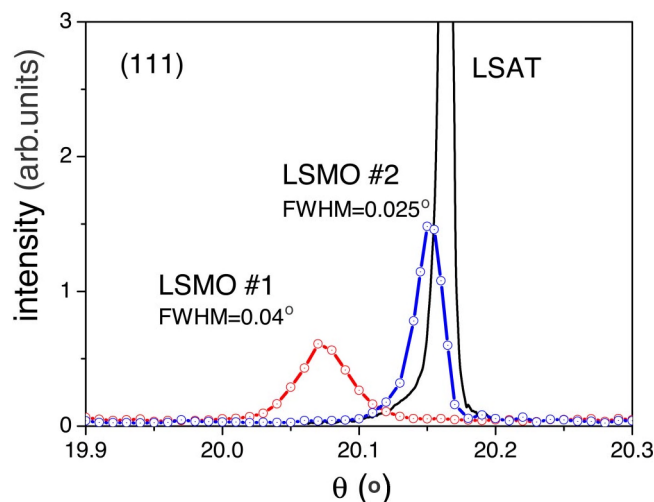


FIG. 1. (Color online.) Rocking curves of the (111) reflex of LSMO No. 1, LSMO No. 2 grown on LSAT. The small FWHM value of both films confirms the good quality.

able, thin films—through strain and imperfections—also serve the purpose of extending the inhomogeneous state to a wider temperature range.

Thin films of LSMO were prepared by using a standard pulsed laser deposition technique.¹⁴ The thickness is 300 nm for LSMO No. 1 and 400 nm for LSMO No. 2. Both were grown onto $(\text{LaAlO}_3)_{0.3}(\text{Sr}_2\text{AlTaO}_5)_{0.7}$ (LSAT). The reflectivity measurements were carried out between 50 cm^{-1} and 40 000 cm^{-1} with the Fourier transform spectrometers Bruker IFS 113v and IFS 66v/S. Careful determination of the optical conductivity σ was achieved by using results of a submillimeter interferometer for the low-energy range in the Kramers-Kronig analysis. Detailed information are published elsewhere.¹¹ The dc resistivity was measured in a four-point configuration. Magnetization measurements were carried out with a commercial Quantum Design SQUID magnetometer for both films and a single crystal.

X-ray diffraction (XRD) measurements were performed using a Bruker D8 Discover four circle x-ray diffractometer. θ - 2θ XRD patterns display no indications of any impurity phase and only (100) diffraction peaks are visible¹³ indicating that the c axis is perpendicular to the substrate surface. In bulk form, LSMO has a rhombohedral structure (space group $R\bar{3}c$). In fact, the average structure can be considered as a slightly distorted cubic perovskite. Hence, we keep the simple cubic notation in the following.

In Fig. 1 we show the out-of-plane rocking curves of the (111) peak for LSMO No. 1, LSMO No. 2, and LSAT. The narrow full width at half maximum (FWHM) of 0.025° for LSMO No. 2 and of 0.04° for LSMO No. 1 indicates the good crystallographic quality and a highly textured crystal growth for both films. The rocking curve measurements characterize information on the angular distribution of the LSMO crystallites in the film. Thus, the lower value of the FWHM of LSMO No. 2 translates into a higher optical conductivity. The quality of the films is slightly different. This is also evidenced by the χ angle of 55.14° and 54.34° for LSMO No. 1 and LSMO No. 2, respectively.

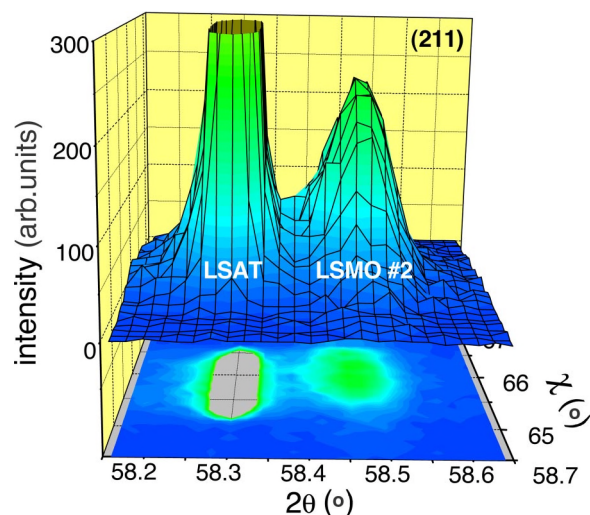


FIG. 2. (Color online.) 3d plot of the (211) reflex of LSAT (substrate) and the LSMO No. 2 film. The bottom plane shows a contour plot of the 2θ - χ space.

The mapping of the (211) reflex for LSMO No. 2 in Fig. 2 is indicative of its good crystal quality. The substrate LSAT and the film peak are well resolved. The extension in the 2θ - χ space for LSMO is only somewhat larger than for the single crystalline substrate.

At low temperature long-range ferromagnetic ordering supports the metallic state. With increasing temperature the FIR optical conductivity σ diminishes up to the metal-insulator transition at T_{MIT} . Figure 3 displays σ in the energy range of the phononic excitations for LSMO No. 2 (lines) and LSMO No. 1 (open circles). We identify eight peaks of transverse optical (TO) phonon modes, corresponding to all

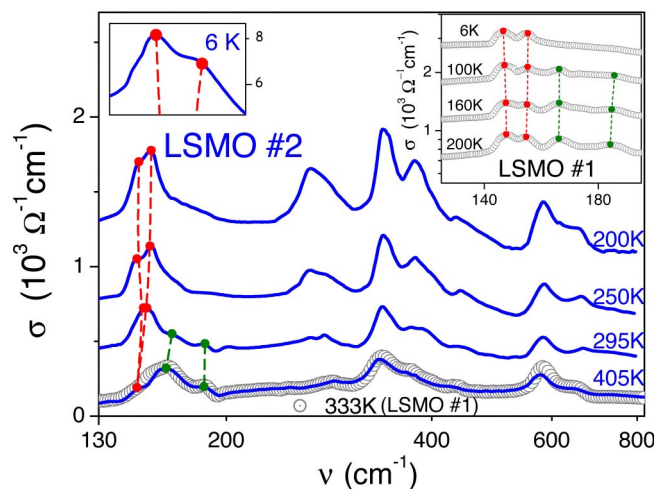


FIG. 3. Temperature-dependent optical conductivity (σ) spectra of LSMO No. 2 (solid lines), with a spectral resolution $\sim 1 \text{ cm}^{-1}$ on a logarithmic frequency scale. We found similar spectra for LSMO No. 1 (open circles at 333 K and right inset), except for a reduction of the respective absolute values and a slightly reduced temperature scale for the evolution of the external modes. The vertical lines connect the maxima of the external modes. Left inset: At 6 K the splitting of the external modes is strongest.

TABLE I. Correspondence between calculated (Ref. 15) and measured phonon modes (LSMO No. 2) for the space group $R3c$ (in cm^{-1}) at $T=405$ K. The values in parenthesis refer to neutron scattering results (Ref. 16) on a $\text{La}_{0.7}\text{Sr}_{0.3}\text{MnO}_3$ single crystal.

calculated			measured	
A_{2u}	E_u	assignment	A_{2u}	E_u
	317	vibration (Mn)		373
162	180	external	150	150
310	357	bending	338 (336)	436 (424)
641	642	stretching	580 (576)	650
	240	torsional		285

IR active vibrations from $R3c$ symmetry. In Table I we present a comparison between the experimental values of the infrared-active phonon frequencies of LSMO No. 2 at $T=405$ K and the calculated frequencies for pure rhombohedral LaMnO_3 by Abrashev *et al.*¹⁵ The calculated positions for the undoped compound should be taken as a rough estimate for LSMO since the lattice constants and atomic positions are modified by doping. Several eigenfrequencies are known from neutron-scattering measurements which are in good agreement with our data.¹⁶

A particular temperature dependence of the mode frequency is observed for the external modes. With increasing temperature the two external modes approach each other and the merged modes shift to lower frequency above $T_C \approx 345$ and 310 K for LSMO No. 2 and LSMO No. 1, respectively (see Fig. 3). A degeneracy of modes indicates a higher lattice symmetry. Moreover, two new modes appear, pointing to a lower lattice symmetry. The new modes gain weight for temperatures close to T_C so that they dominate the group of external modes above T_C . This phenomenon of phonon metamorphosis is observable in both films, in LSMO No. 2 as well as in LSMO No. 1 (see open circles in Fig. 3). The groups of stretching and bending modes are weakly affected by the ferromagnetic to paramagnetic transition except for the torsional mode at about 285 cm^{-1} which is shifted to higher frequencies.

The external group is displayed in Fig. 4 on an enlarged scale. The two new modes at approximately 169 and 186 cm^{-1} are referred to as ν_3 and ν_4 , respectively. The selected temperatures fully cover the interval in which both, the magnetic and the metal-to-insulator transition, take place ($T_C \approx 345$ K and $T_{\text{MIT}} \approx 401$ K). The presumption that the evolution of these modes is controlled by the spin DOF is substantiated by the temperature analysis of the mode frequencies. The temperature dependence of the splitting of the low-frequency pair of modes $\Delta\nu$ is presented in Fig. 5 (left panel, full circles). The solid line is the normalized magnetization $[M(T)/M(0)]$. Although no theoretical modeling is available to relate magnetization and mode splitting quantitatively, the observation that M and $\Delta\nu$ drop on the same temperature scale T_C to zero suggests a correlation between spin polarization and these phonon modes. A similar observation is found for the temperature dependence of the mode frequencies ν_3 and ν_4 . The relevant temperature scale is

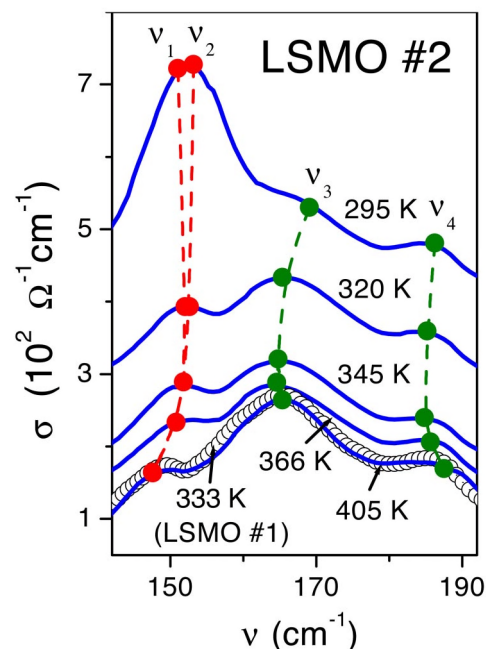


FIG. 4. Metamorphosis of phonon modes: optical conductivity σ of the external modes (ν_1, ν_2) and the new modes (ν_3, ν_4). The latter modes are absent at low temperatures. With increasing temperature, spectral weight is transferred from the low-energy external group to the new modes (see Fig. 6).

clearly T_C , and not T_{MIT} , as shown for $\nu_3(T)$ in the right panel of Fig. 5. Neutron-scattering measurements^{17,18} show that the structural distortion does not change at T_C and thereby confirm that neither the lattice structure nor the thermal expansion of the lattice can be attributed to the temperature behavior of the external modes in the vicinity of T_C . It is suggestive to relate the observed phonon metamorphosis to the formation of an inhomogeneous state, as this state may support two types of external modes. The spectral weight transfer from the modes ν_1 and ν_2 to the “new modes” ν_3 and ν_4 (see Fig. 6) accentuates the crossover into the inhomogeneous state at a temperature well below T_{MIT} .

In order to confirm that we indeed observe an intrinsic inhomogeneous state, which is controlled by the temperature scale T_C , we also investigated the susceptibility of these

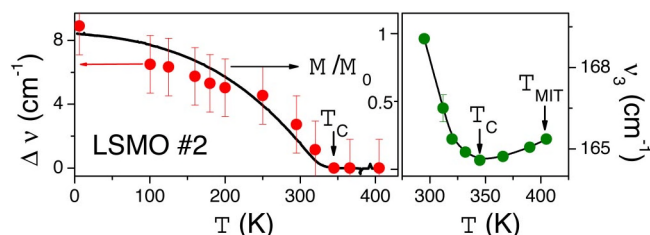


FIG. 5. Left panel: Splitting $\Delta\nu = \nu_2 - \nu_1$ between the eigenfrequencies of the two external modes at various temperatures (full circles). The solid line is the temperature dependent magnetization of LSMO No. 2. Right panel: Temperature dependence of the frequency of the new mode ν_3 . At T_C the direction of the shift is reversed. Beyond T_{MIT} the phonon spectrum is invariant with respect to T .

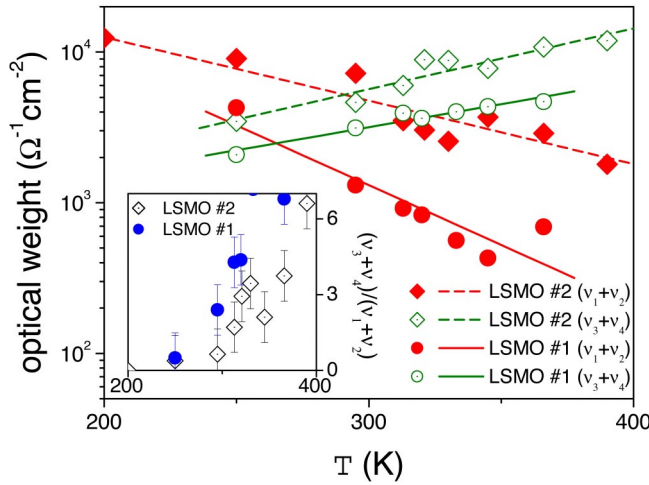


FIG. 6. Temperature dependence of the optical weight of the external modes for LSMO No. 2 and LSMO No. 1. ($\nu_1 + \nu_2$) refers to the weight of the original external modes while ($\nu_3 + \nu_4$) applies to the new modes. The inset displays the ratio of the optical weight of the new modes to that of the original modes.

LSMO films in low magnetic fields. Salamon and Chun¹⁹ could not detect the onset of a Griffiths-like phase for $\text{La}_{0.7}\text{Sr}_{0.3}\text{MnO}_3$ single crystals. However, thin films are intrinsically more inhomogeneous and the question arises if they display Griffiths singularities. In fact, our measurements of the susceptibility χ of LSMO No. 2 (400 nm film) and LSMO No. 1 (300 nm film) in Fig. 7 support such a scenario. Whereas the single crystal with the same Sr concentration shows the conventional Curie-Weiss behavior with an effective magnetic moment $p_{\text{eff}} = 5.1 \mu_B$ (open circles), the films display a sharp downturn in $\chi^{-1}(T)$ at a temperature $T^* \sim 370$ K above their respective Curie temperatures $T_C^{\text{No. 1}} = 310$ K and $T_C^{\text{No. 2}} = 345$ K. The onset T^* is similar for both films and corresponds to the Curie temperature $T_C \sim 370$ K of the single crystal. Such a behavior may be interpreted in

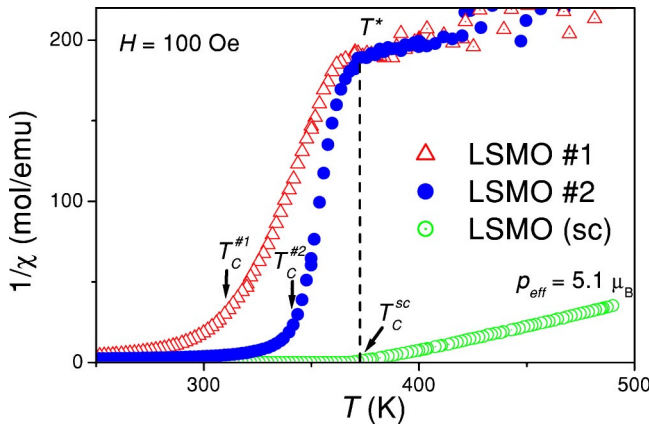


FIG. 7. Temperature dependence of the low-field inverse magnetic susceptibility for three samples (LSMO (sc): single crystal, LSMO No. 2 and LSMO No. 1). Arrows indicate T_C from magnetization measurements. The effective magnetic moment p_{eff} in the paramagnetic phase slightly above T^* is approximately $5 \mu_B$ for all samples (Ref. 20).

terms of a Griffiths-like phase, where the enhanced disorder in the films, in comparison to the single crystal, accounts for the reduced T_C and for the formation of inhomogeneous magnetic states below $T^* \sim T_C^{\text{sc}}$.

Whereas the non-Curie-Weiss behavior of the susceptibility points to the existence of spin clusters in the films, it does not predict the lower temperature at which an inhomogeneous state first develops. Probably “electronic phase separation between phases with different densities on a nano scale”²⁴ is established before the disorder-induced Griffiths-like phase for the spin system sets in. Even if the underlying model were known, it would be difficult to make conclusive predictions as the phase separation in these systems seems to be dynamic.²¹

We conclude the paper with a discussion of the origin of the new modes. We suggest that the observed phonon metamorphosis is to be understood in the context of a T -dependent, inhomogeneous dynamical Jahn-Teller distortion (IDJT). The IDJT is probed by distinct phonon excitations which “sense” the inhomogeneities as soon as the charge carriers slow down with increasing temperature and the lattice DOF experience a crossover from adiabatic to nonadiabatic behavior.

Louca and Egami¹⁰ investigated deviations of the local structure from the average crystal structure in $\text{La}_{1-x}\text{Sr}_x\text{MnO}_3$ by pulsed neutron scattering with pair distribution function analysis (PDF) and Shibata *et al.*²² with x-ray absorption fine structure (XAFS). With these findings the tentative scenario for the merging of two phonons and the formation of new modes is as follows:

At low temperatures, deep in the metallic phase, the dynamics of the mobile charge carriers is fast with respect to the lattice DOF: the lattice reacts on the average charge carrier concentration, not on the instantaneous hole positions. In this regime, only a weak dynamical JT distortion is observed and the external modes are split as seen for the 6 K line shape of the inset of Fig. 3. For increasing temperature, the charge carrier dynamics is slower since the double exchange mechanism is less effective and the overall picture becomes more local. A finite-size polaron emerges which is, according to Louca and Egami, rather an “antipolaron” where the lattice around the slower holes is locally less and less JT distorted. Correspondingly, the splitting of the external modes is reduced. The weight of these phonon resonances decreases because sites without antipolarons experience a strong JT distortion and support external modes at a higher frequency (as is well known from the undoped or weakly doped systems^{23–25}). These “new external modes” at higher frequency also experience a larger splitting, again consistent with the observations in undoped or weakly doped systems. We refer to this situation as the temperature dependent IDJT. The basis for the observation of the IDJT is a crossover from adiabatic to nonadiabatic behavior of the lattice dynamics.

To conclude, we emphasize the particular importance of the external modes as an excellent phononic “tool” to investigate the cooperative behavior of the lattice with spin and charge DOF. These phonons have a weak dispersion¹⁶ which allows them to probe local distortions. Moreover, the frequency shift of the external modes is strong with Sr doping because these modes correspond to a vibration of the La—Sr

cage with respect to the Mn—O octahedra. For this reason the low-energy modes of the external group are well separated from the new modes at high temperature. The disentanglement of the external modes in the electronic inhomogeneous state is the prerequisite of the observed phonon metamorphosis.

We thank D. Braak for an introduction into the physics of

Griffiths-McCoy singularities. X-ray measurements were performed at the Walther-Meissner-Institut (Garching). Assistance by A. Erb and P. Majewski is gratefully acknowledged. The research was supported in part by BMBF (Grant Nos. 13N6917A, 13N6918A), by the DFG via SFB 484 (Augsburg), and by the DAAD, Grant No. D/03/36760.

-
- ¹A. J. Millis, P. B. Littlewood, and B. I. Shraiman, Phys. Rev. Lett. **74**, 5144 (1995).
²M. Uehara, S. Mori, C. H. Chen, and S.-W. Cheong, Nature (London) **399**, 560 (1999).
³A. Moreo, S. Yunoki, and E. Dagotto, Science **283**, 2034 (1999).
⁴E. Dagotto, T. Hotta, and A. Moreo, Phys. Rep. **344**, 1 (2001).
⁵M. B. Salamon, P. Lin, and S. H. Chun, Phys. Rev. Lett. **88**, 197203 (2002).
⁶R. B. Griffiths, Phys. Rev. Lett. **23**, 17 (1969).
⁷E. Dagotto, *Nanoscale Phase Separation and Colossal Magnetoresistance* (Springer, Berlin 2002).
⁸M. Fäth, S. Freisem, A. A. Menovsky, Y. Tomioka, J. Aarts, and J. A. Mydosh, Science **285**, 1540 (1999).
⁹T. Becker, C. Streng, Y. Luo, V. Moshnyaga, B. Damaschke, N. Shannon, and K. Samwer, Phys. Rev. Lett. **89**, 237203 (2002).
¹⁰D. Louca and T. Egami, Phys. Rev. B **59**, 6193 (1999).
¹¹Ch. Hartinger, F. Mayr, A. Loidl, and T. Kopp, Phys. Rev. B **70**, 134415 (2004).
¹²Ch. Hartinger, F. Mayr, J. Deisenhofer, A. Loidl, and T. Kopp, Phys. Rev. B **69**, 100403(R) (2004).
¹³Ch. Hartinger, F. Mayr, A. Loidl, and T. Kopp, cond-mat/0406123 (unpublished).
¹⁴D. Christey and G. Hubler, *Pulsed Laser Deposition of Thin Films* (Wiley, New York, 1994).
¹⁵M. V. Abrashev, A. P. Litvinchuk, M. N. Iliev, R. L. Meng, V. N. Popov, V. G. Ivanov, R. A. Chakalov, and C. Thomsen, Phys. Rev. B **59**, 4146 (1999).
¹⁶W. Reichardt and M. Braden, Physica B **263**, 416 (1999).
¹⁷M. C. Martin, G. Shirane, Y. Endoh, K. Hirota, Y. Moritomo, and Y. Tokura, Phys. Rev. B **53**, 14 285 (1996).
¹⁸A. Møllergård, R. L. McGreevy, and S. G. Eriksson, J. Phys.: Condens. Matter **12**, 4975 (2000).
¹⁹M. B. Salamon and S. H. Chun, Phys. Rev. B **68**, 014411 (2003).
²⁰As a consequence of the imprecise mass determination of thin films the scale of $\chi^{-1}(T)$ is subject to some uncertainty.
²¹R. H. Heffner, J. E. Sonier, D. E. MacLaughlin, G. J. Nieuwenhuys, G. Ehlers, F. Mezei, S.-W. Cheong, J. S. Gardner, and H. Röder, Phys. Rev. Lett. **85**, 3285 (2000).
²²T. Shibata, B. A. Bunker, and J. F. Mitchell, Phys. Rev. B **68**, 24 103 (2003).
²³A. Paolone, P. Roy, A. Pimenov, A. Loidl, O. K. Melnikov, and A. Ya. Shapiro, Phys. Rev. B **61**, 11 255 (2000).
²⁴V. B. Podobodov, A. Weber, D. B. Romero, J. P. Rice, and H. D. Drew, Phys. Rev. B **58**, 43 (1998).
²⁵In $\text{La}_{0.95}\text{Sr}_{0.05}\text{MnO}_3$ the resonances of the external modes are at 169 and 180 cm^{-1} for room temperature.